Asian Journal of Chemistry; Vol. 38, No. 1 (2026), 107-113
ASIAN JOURNAL OF CHEMISTRY
https://doi.org/10.14233/ajchem.2026.34881

Enhanced Electrochemical Detection of Ambroxol Using AgNPs/MWCNT/Nafion/GCE Composite Sensor

RIDDHI TRIVEDI*, and PRAJESH PRAJAPATI

School of Pharmacy, National Forensic Sciences University, Gandhinagar-382007, India

*Corresponding author: E-mail: riddhi.trivedi@nfsu.ac.in

Received: 11 September 2025 *Accepted*: 11 November 2025 *Published online*: 31 December 2025 AJC-22228

The development of the nanocomposite using AgNPs/MWCNT/Nafion/GCE in this study represents a significant advancement in the electrochemical detection of ambroxol, an important therapeutic agent in respiratory medicine. Silver nanoparticles (AgNPs) were green-synthesized using *Hyphaene thebaica* extract and integrated with functionalized multi-walled carbon nanotubes (MWCNTs) in a Nafion matrix to develop a highly sensitive electrochemical sensor for ambroxol. SEM, XRD and FTIR confirmed irregular, crystalline AgNPs strongly capped with phytochemicals, while acid-treated MWCNTs exhibited enhanced dispersibility due to surface carboxylation. The AgNPs/MWCNT/Nafion-modified glassy carbon electrode showed markedly improved electrocatalytic activity, enlarged electroactive surface area and irreversible, diffusion-controlled oxidation of ambroxol. The optimal sensing conditions were obtained at pH 4, 6 µL modifier loading and a 4 min accumulation time. The sensor demonstrated a linear range of 0.01-5 × 10^{-5} M, a detection limit of 6 × 10^{-6} M, high selectivity and excellent reproducibility (RSD 3.6%). Application to spiked urine samples yielded an average recovery of 100.9%, validating its potential for pharmaceutical and clinical analysis.

Keywords: Silver nanoparticles, *Hyphaene thebaica*, Ambroxol, MWCNT, Electrochemical sensor.

INTRODUCTION

Nanocomposite-based sensors have emerged as powerful analytical tools in recent years, particularly for the detection of trace-level pharmaceutical compounds in complex matrices [1-4]. Their enhanced conductivity, high surface area and tunable surface chemistry make them highly suitable for applications requiring sensitivity, selectivity and rapid response [5,6]. Ambroxol, a widely prescribed mucolytic and expectorant agent, was selected as the target analyte in this study due to its extensive use in the management of respiratory disorders characterized by excessive mucus secretion [7-9]. Chemically known as *trans*-4-(2-amino-3,5-dibromophenylmethylamino)cyclohexanol ($C_{14}H_{20}Br_2N_2O$, m.w. 414.56 g/mol), ambroxol is a white to yellowish crystalline compound with limited solubility in water and alcohol. Accurate determination of ambroxol in pharmaceutical formulations and biological fluids is crucial for quality control, pharmacokinetic studies and clinical diagnostics.

Conventional analytical approaches for ambroxol quantification, including high-performance liquid chromatography and UV-visible spectroscopy, although reliable, often require costly instrumentation, laborious-intensive protocols, and complex sample preparation [10,11]. These limitations have driven the demand for simplified, cost-effective and highly sensitive sensing platforms. Electrochemical methods, particularly voltammetric techniques, offer distinct advantages such as rapid analysis, low detection limits, and minimal sample preparation. When coupled with functional nanomaterials, their analytical performance can be significantly enhanced [6,12,13].

In this context, nanocomposites incorporating silver nanoparticles (AgNPs), multi-walled carbon nanotubes (MWCNTs) and Nafion provide a promising route for sensor development. AgNPs exhibit excellent catalytic properties [14,15], MWCNTs offer superior electrical conductivity and large surface area [16] and Nafion functions as an efficient binder providing mechanical stability and uniform dispersion [17]. When assembled onto a glassy carbon electrode (GCE), these components act synergistically to enhance electron transfer kinetics and amplify the electrochemical signal of the target analyte.

The present study focuses on the fabrication and application of an AgNPs/MWCNT/Nafion-modified GCE for the electrochemical detection of ambroxol. The sensor was prepared by ultrasonication-assisted dispersion of MWCNTs in Nafion followed by electrode modification and incorporation of AgNPs. Preliminary results demonstrate a substantial improvement in oxidation peak current compared with bare GCE, confirming the strong electrocatalytic contribution of the nanocomposite. The developed sensor was successfully applied for the determination of ambroxol in commercial tablet formulations and spiked urine samples, highlighting its potential as a reliable, efficient and economically viable analytical tool for pharmaceutical and clinical applications.

EXPERIMENTAL

Biosynthesis of silver nanoparticles (AgNPs): Using an eco-friendly green synthesis approach, AgNPs were prepared with *Hyphaene thebaica* plant extract. A 20 mL of the extract was added to 60 mL of 2 mM $AgNO_3$ solution, resulting in a colour change from light brown to deep dark brown, indicating the formation of AgNPs due to the reducing properties of the plant biomolecules. The mixture was centrifuged at 8000 rpm for 20 min, a process repeated twice to ensure nanoparticle separation and purity. The resulting pellet was evenly spread in petri dishes and dried at 70 ºC for 24 h. The dried nanoparticles were gently collected as a fine powder.

Preparation of MWCNT/Nafion modified GCE: The MWCNT/Nafion-modified glassy carbon electrode (GCE) was prepared by first thoroughly clean the GCE to remove any surface contaminants. A precise 6 µL of MWCNT/Nafion suspension was then applied to the electrode surface to form a uniform, thin film, followed by air drying to ensure stable film formation.

Fabrication of AgNPs/MWCNT/Nafion/GCE composite sensor: The previously prepared AgNPs and functionalized MWCNTs were dispersed in a Nafion solution to form a homogeneous composite, with Nafion acting as a matrix for uniform distribution. The mixture was ultrasonicated to ensure even dispersion, critical for sensor performance and surface coverage. The GCE was thoroughly cleaned using alumina slurry, followed by sonication in distilled water and ethanol (or acetone) and finally rinsed with water. A precise volume of the AgNPs/MWCNT/Nafion composite was dropcast onto the GCE surface, ensuring adequate coverage without forming an overly thick film. The electrode was then air-dried or gently dried under nitrogen to remove the solvent while maintaining uniform nanoparticle and nanotube distribution [9].

Characterization of AgNPs: Characterization of AgNPs was done utilizing UV-visible spectrophotometer, Shimadzu 1900i at 25 ºC. The surface topography was characterized by scanning electron microscope (SEM) Zeiss EVO 18, at 5 kV. X-ray diffraction (XRD) was performed on a Bruker D8 Focus instrument, wavelength (λ = 1.54 Å). The Fourier infrared was recorded by QATRS-IR, Shimadzu IRSpirit-L spectroscopy and the spectra were obtained at range of 4000-400 cm^{-1}.

Electrochemical analysis: The electrochemical detection of ambroxol was evaluated using a Metrohm analyzer with a three-electrode system comprising a glassy carbon electrode (GCE) modified with MWCNT/Nafion and AgNPs as working electrode, platinum wire as counter and Ag/AgCl as reference. Initial analysis with a carbon paste electrode (CPE) showed high oxidation potential, low peak current and a limited linear range. The bare GCE improved the response, but the AgNPs/MWCNT/Nafion-modified GCE exhibited the most significant enhancement, with a well-defined oxidation peak at lower potential and higher current, demonstrating superior electrocatalytic activity and electron transfer. Ambroxol displayed irreversible behaviour, as no reduction peak was observed. Electrode regeneration through multiple cyclic scans yielded stable voltammograms. Comparative cyclic voltammetry (0.001 M ambroxol) confirmed peak current enhancement at AgNPs/MWCNT/Nafion/GCE compared to bare and Nafion-modified GCE. Surface area calculations using the Randles-Sevcik equation showed an increase from 0.0828 cm^2 (bare GCE) to 0.135 cm^2 (modified GCE), indicating successful modification and enhanced electrochemical activity.

RESULTS AND DISCUSSION

Characterization of AgNPs: The SEM micrographs (Fig. 1) revealed that the green synthesized AgNPs are irregular in shape. The phytochemicals present in the plant extract, owing to their strong reducing ability toward Ag^+ ions, promoted controlled nucleation of silver nuclei, resulting in a relatively narrow size distribution [18]. These phytochemicals likely adsorbed onto the nanoparticle surfaces, stabilizing the AgNPs and facilitating further nucleation. Their affinity for Ag^+ ions plays a critical role in determining nucleation, growth behaviour and the final size distribution of the AgNPs [19]. The SEM images also indicate that the AgNPs are coated with layers of phytochemical compounds from the plant extract. These capping layers contribute to particle stabilization and influence the physical morphology of the nanoparticles.

XRD analysis was performed to examine the crystalline structure of the synthesized AgNPs (Fig. 2). Several distinct Bragg diffraction peaks were observed at 2θ values of 27.81º, 32.16º, 38.12º, 44.30º, 46.21º, 54.83º, 57.39º, 64.42º and 77.45º. These peaks correspond to the characteristic reflections of pure silver with a face-centered cubic (fcc) crystal structure (JCPDS card No. 04-0783) [20]. The calculated *d*-spacings were consistent with the fcc phase of metallic silver and the sharpness of the diffraction peaks indicates high crystallinity of the AgNPs. These results clearly confirm that the silver nanoparticles synthesized using the plant extract are crystalline in nature.

FTIR spectrum (Fig. 3) provided the involvement of plant metabolites in reducing and stabilizing AgNPs. The plant extract exhibited the characteristic vibrational bands between 1600-700 cm^{-1} and 3400-3000 cm^{-1}, corresponding to aromatic ring modes, C–O stretching of phenols/ethers, O–H bending, and C=C/C=O stretching of polyphenolic and flavonoid structures [21]. These peaks confirm that compounds such as tannins, phenols, flavonoids, terpenoids, saponins and glycosides act as both reducing and capping agents, altering their electronic environment upon coordination with AgNPs surfaces. Interestingly, the absence of a distinct band near ~877 cm^{-1} typically associated with Ag–O vibrations suggests that

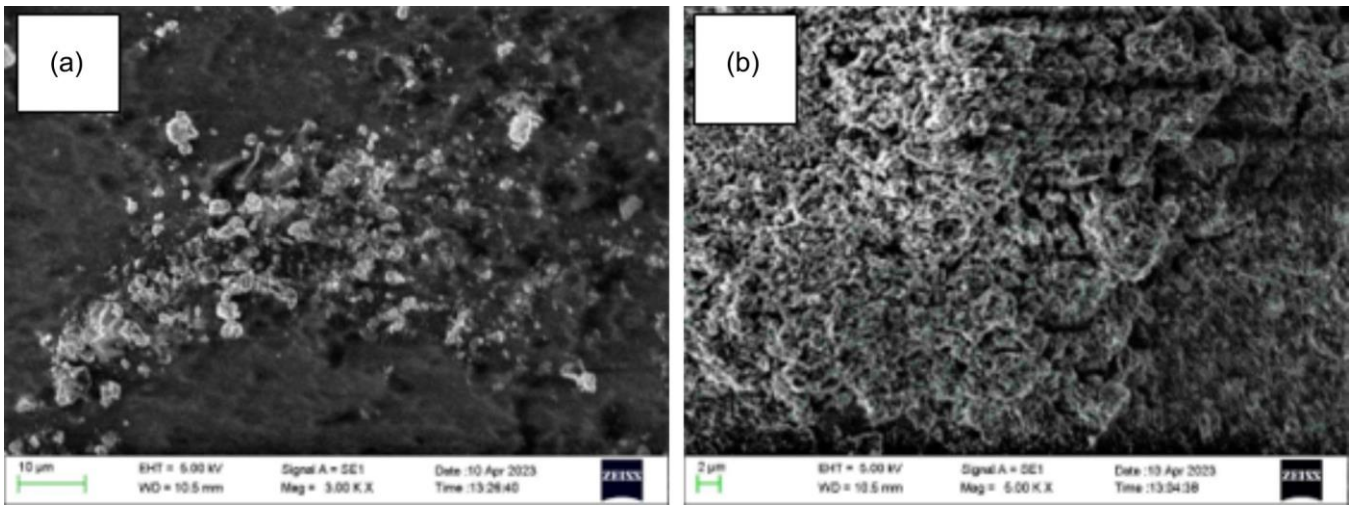

Fig. 1. SEM images of synthesized AgNPs at 3000X (a) and 5000X (b) magnifications

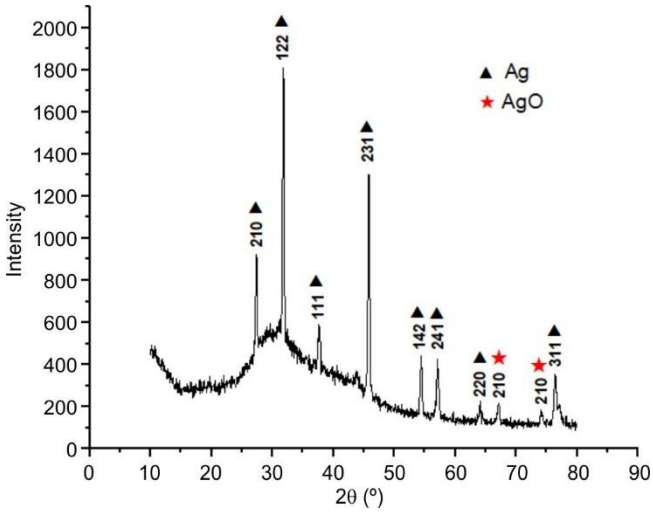

Fig. 2. XRD pattern of synthesized AgNPs

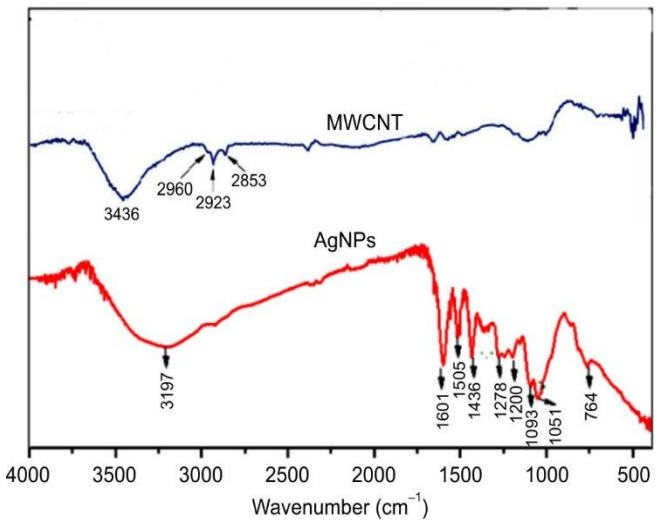

Fig. 3. FTIR spectra of MWCNT and AgNPs

any metal–oxygen interactions are masked by the dense organic coating [22]. This is consistent with reports where strong phytochemical adsorption screens metal–oxygen vibrational signatures, even when XRD confirms oxidation states or lattice formation. Thus, the significant shifts in peak positions and changes in intensity within these regions suggest strong chemisorption of these functional groups onto the metal surface.

Additional FTIR peaks corresponding to the MWCNT component of the composite further support successful material integration. The appearance of the G-band (~1580 cm^{-1}) and D-band (~1350 cm^{-1}) confirms the presence of sp^2-carbon frameworks and structural disorders typical of oxidized or functionalized nanotubes [23,24]. The bands at 2960 and 2923 cm^{-1}, attributed to the C–H stretching of methyl and methylene groups, indicate surface functional groups likely generated during oxidative pretreatment or through interactions with Nafion and phytochemicals [25]. Together, these spectral features demonstrate that the MWCNTs are not merely physically mixed but are chemically modified and well-dispersed, enabling enhanced electron mobility and synergistic interaction with the AgNPs are the critical factors for the amplified electrochemical response of the sensor.

Electrochemical analysis: A comparative study revealed that the AgNPs/MWCNT/Nafion-modified GCE significantly outperformed both Nafion/GCE and bare GCE. Cyclic voltammetry demonstrated enhanced peak currents at the modified electrode, in contrast to poorly defined peaks observed at the bare GCE. Plotting the peak current against the square root of the scan rate for AgNPs/MWCNT/Nafion/GCE showed a strong linear relationship, with a slope of 0.17 and an R^2 value of 0.9791 (Fig. 4a), whereas the bare GCE exhibited a slope of 0.13 and R^2 = 0.9985 (Fig. 4b), indicating the lower responsiveness. Using the Randles-Sevcik equation [26], the effective surface area of the AgNPs/MWCNT/Nafion/GCE (0.135 cm^2) was considerably higher than that of the bare GCE (0.0828 cm^2). This increase in surface area corresponds to a more active electrode surface, enhancing electrochemical activity and sensitivity. Incorporation of AgNPs and MWCNTs into the Nafion matrix markedly improved the electroactive surface area, facilitating more efficient electrochemical detection of ambroxol. These results highlight the critical role of electrode surface modification in developing sensitive and effective electrochemical sensors for pharmaceutical analysis.

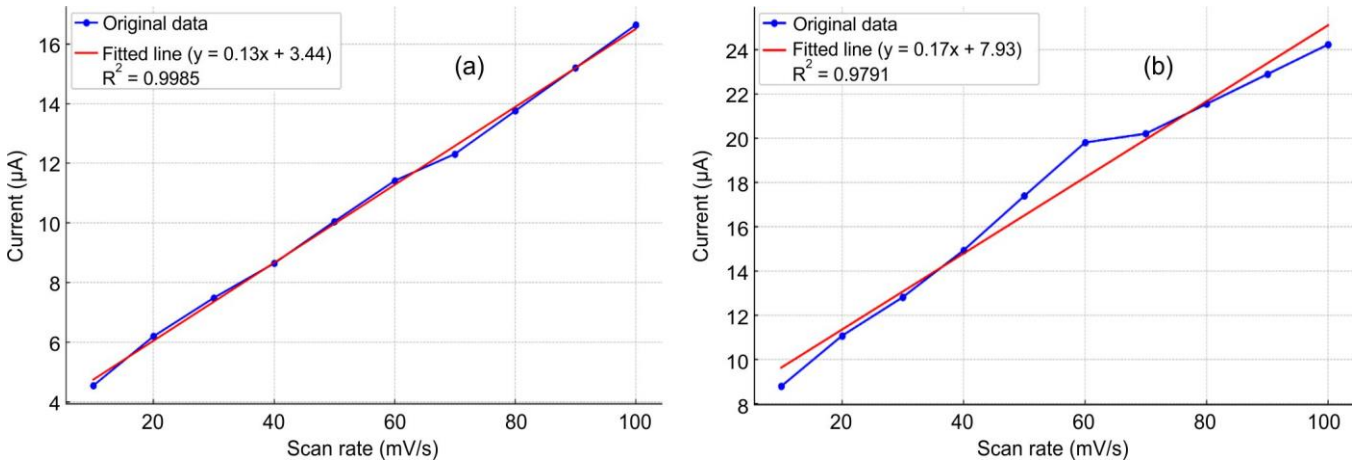

Fig. 4. Current and scan-rate of bare GCE (a) and AgNP/MWCNT/Nafion/GCE (b) using 2 mM $K_3[Fe(CN)_6]$

Furthermore, linear regression analysis of the surface area for the bare GCE using a 2 mM $K_3[Fe(CN)_6]$ solution yielded a slope of 0.1307 μA/(mV/s) and an intercept of 3.4355 μA, with R^2 = 0.9985. The strong linearity confirms that the electrochemical process at the bare GCE is diffusion-controlled and the electrode behaviour can be reliably analyzed under the experimental conditions.

Effect of pH: The influence of pH on the electrochemical response of ambroxol was investigated using a three-electrode system comprising the AgNPs/MWCNT/Nafion-modified GCE as the working electrode, a platinum wire as the counter electrode and an Ag/AgCl reference electrode. The cyclic voltammetry (CV) measurements were conducted across a pH range of 2-9 using 1×10^{-3} M ambroxol, with the solution purged with nitrogen prior to each run to remove oxygen interference. Fig. 5 demonstrated a clear dependence of the sensor's response on pH. The anodic peak current was maximal at pH 4, reaching 25 μA, indicating the optimal electrochemical environment for ambroxol oxidation and the ideal operating condition for selective and efficient detection. At higher pH values, the sensor performance decreased significantly: the peak current dropped to 5 μA at pH 7 and further declined to 0.5 μA at pH 9. This reduction is likely due to ambroxol deprotonation and changes in its electrochemical kinetics at alkaline conditions, which adversely affect sensor response [27]. Overall, the data clearly identifies pH 4 as the optimal condition for the AgNPs/MWCNT/Nafion-modified GCE, providing crucial guidance for the effective electrochemical detection of ambroxol in analytical applications.

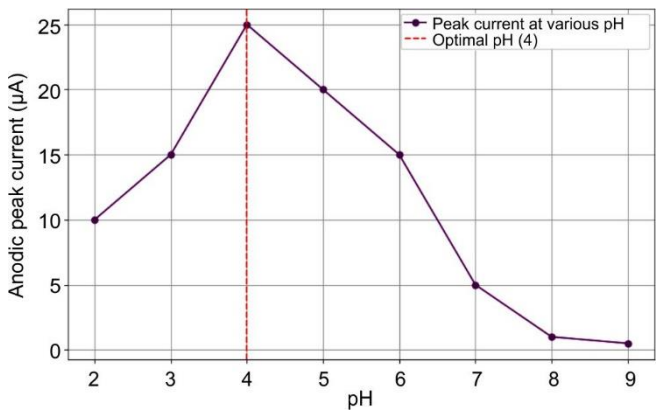

Fig. 5. Effect of pH on anodic peak current

Effect of amount of AgNPs/MWCNT-Nafion dispersion: The effect of the amount of AgNPs/MWCNT/Nafion dispersion on sensor performance was evaluated by applying varying amounts onto the cleaned GCE surface. The results showed that increasing the dispersion volume up to 6 μL led to a corresponding increase in the anodic peak current for 1×10^{-3} M ambroxol, indicating enhanced electron transfer, a larger electroactive surface area and more accessible catalytic sites (Fig. 6a-b). Beyond 6 μL, a slight decrease in peak current was observed, likely due to excessive AgNPs/ MWCNT electrode causing surface congestion. This overcrowding can hinder electron transfer by forming a diffusion barrier or altering the local environment at the electrode surface. Therefore, 6 μL of AgNPs/MWCNT/Nafion dispersion was established as the ideal volume for achieving maximum sensor response without compromising efficiency.

Effect of accumulation time and scan rate: The influence of accumulation time on the voltammetric response of 1×10^{-3} M ambroxol was investigated to optimize the pre-concentration step. Measurements were performed at open-circuit potential without stirring, and the anodic peak current was monitored over time (Fig. 7a). The peak current increased over the first 4 min and then stabilized, indicating that the electrode surface became saturated with ambroxol. And also suggested that 4 min is the optimal accumulation time for the effective pre-concentration on the AgNPs/MWCNT/Nafion-modified GCE.

The effect of scan rate was also studied at scan rates ranging from 50 to 250 mV/s using linear sweep voltammetry (LSV) on the modified electrode. The anodic peak current increased with increasing scan rate and a linear relationship was observed between the peak current and the square root of the scan rate (Fig. 7b), consistent with a diffusion controlled electrochemical process as described by the Randles-Sevcik equation [28]. In addition, the broadening of peaks and slight shifts in peak potential at higher scan rates provide insight into the kinetics and reversibility of the oxidation process of ambroxol. These observations confirm that the electrochemical

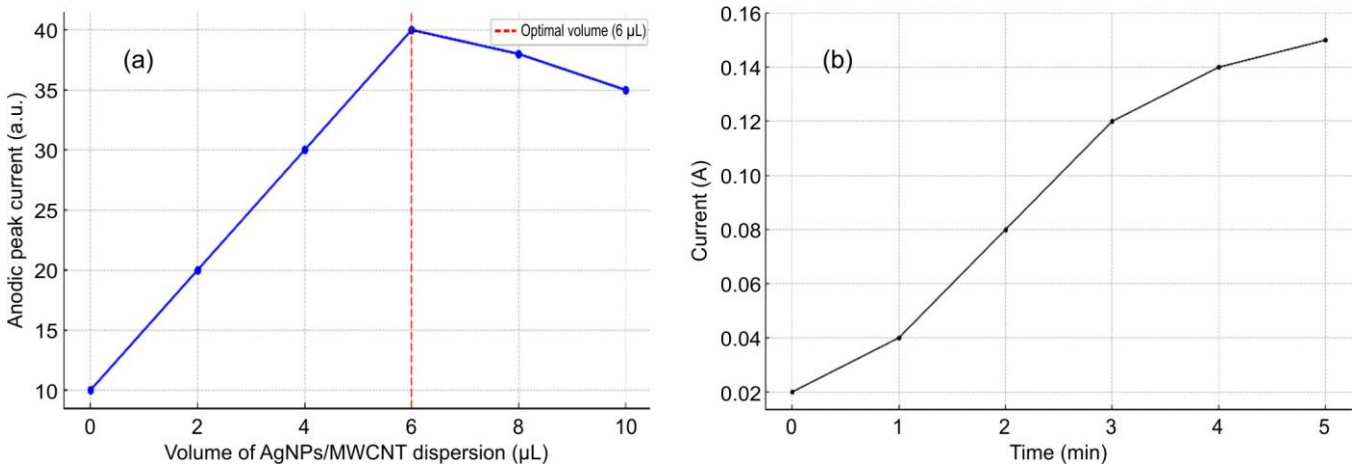

Fig. 6. Effect of amount of AgNP/MWCNT-Nafion dispersion

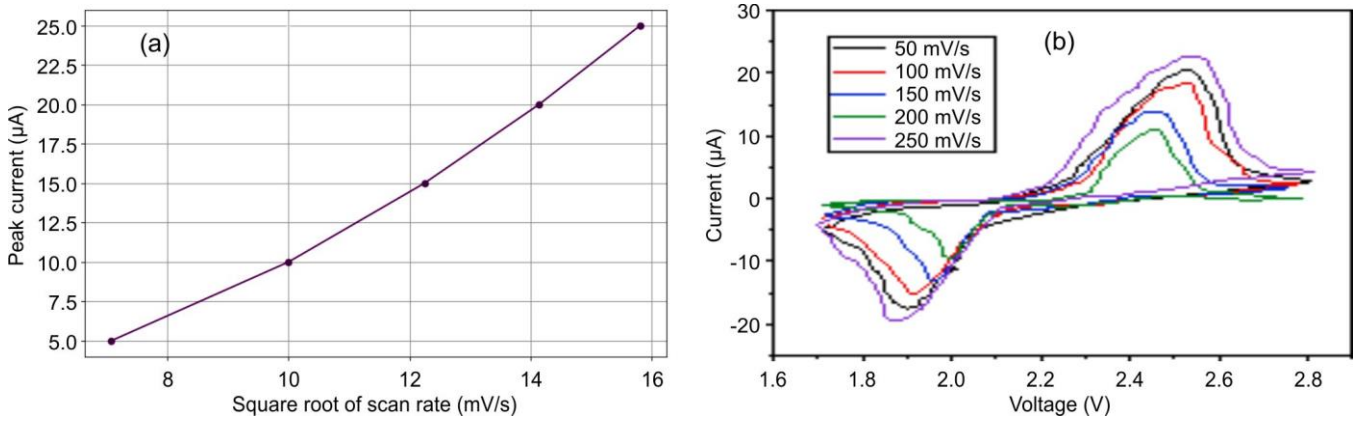

Fig. 7. (a) Graph demonstrates a linear relationship between the square root of the scan rate and peak current, indicating a diffusion-controlled electrochemical process as per the Randles-Sevcik equation and (b) Cyclic voltammograms at varying scan rates show broader peaks and increased peak currents as the scan rate increases, consistent with diffusion-controlled processes

response is governed by diffusion of ambroxol to the electrode surface and that the optimized accumulation time and understanding of scan rate effects are essential for maximizing sensor sensitivity and reproducibility.

Calibration curve and detection limit: The relationship between the anodic peak current and ambroxol concentration was evaluated using linear sweep voltammetry (LSV). The AgNPs/MWCNT/Nafion-modified GCE sensor exhibited a linear working concentration range from 5×10^{-5} to 1×10^{-2} M. At very low concentrations, the sensitivity of the proposed sensor decreased, with a detection limit determined to be 1×10^{-6} M (Fig. 8). The sensor demonstrated excellent reproducibility: repeated measurements of 1×10^{-3} M ambroxol, with the electrode surface regenerated between tests, showed minimal variation, with a relative standard deviation of ±3.6%. These results confirm the reliable performance of the sensor, wide working range and suitability for precise electrochemical detection of ambroxol.

Interference study and selectivity: The selectivity of the AgNPs/MWCNT/Nafion-modified GCE sensor was evaluated in the presence of various organic and inorganic compounds. Using a 5×10^{-5} M ambroxol solution, a 100-fold excess of substances such as glucose, fructose, Na^+, K^+, Cl^-, SO_4^{2-}, glutamic acid, lactose, citric acid and urea caused

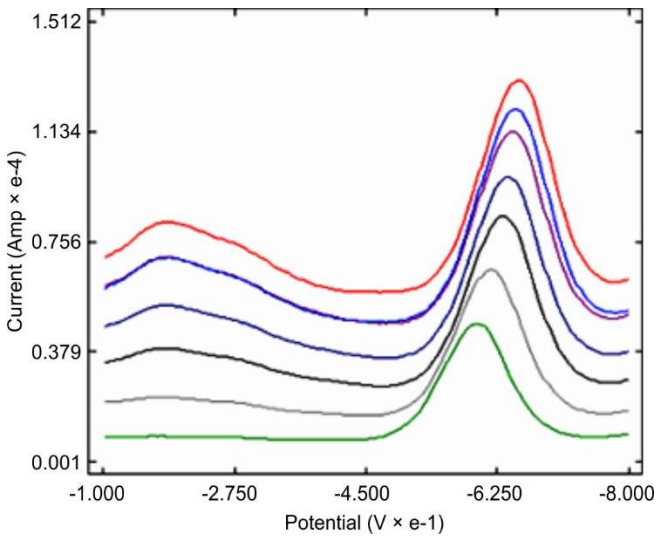

Fig. 8. Linear sweep voltammetry of the relationship between the anodic peak current of ambroxol

minimal changes in the oxidation peak current, generally below 5%, demonstrating high selectivity (Table-1). Detailed observations showed that lactose produced a 0.737% signal change, Na^+ and Cl^- decreased the current by 4.378%, K^+ and

TABLE-2
DETERMINATION OF AMBROXOL IN TABLETS

Sample	Method	Amount (mg/tablet)	Found (mg/tablet)	S.D.	C.V.
Ambroxol HCl	Present developed sensor	30	30.5	0.902	3.003
Ambroxol HCl	Standard method	30	31.9	1.111	3.531

*Average of six replicates

TABLE-1
STUDY ON THE EFFECT OF FOREIGN SPECIES ON THE OXIDATION PEAK CURRENT OF 0.0005 M AMBROXOL

Substance	Concentration (M)	Current (mA)	Signal change (%)
Ambroxol	0.0005	0.031500	–
Lactose	0.01	0.031290	0.737
Na^+	0.01	0.030345	4.378
Cl^-	0.01	0.030345	4.378
K^+	0.01	0.030450	3.663
SO_4^{2-}	0.01	0.030450	3.663
Glutamic acid	0.01	0.032760	4.004
Ascorbic acid	0.01	0.028665	10.23
Glucose	0.01	0.030135	5.137
Citric acid	0.01	0.030870	2.563
Fructose	0.01	0.028500	4.500
Urea	0.01	0.030100	0.330

SO_4^{2-} caused a 3.66% decrease, and glutamic acid slightly increased the peak current by 4.00%. Glucose and fructose altered the signal by 5.14% and 4.50%, respectively, while citric acid induced a moderate decline of 2.56% and urea had the least effect (0.33%). In contrast, ascorbic acid caused the largest interference, reducing the peak current by 10.23%, indicating a notable limitation in samples containing this compound. These findings underscore the high selectivity of the sensor for ambroxol while highlighting the importance of considering potential interfering substances in real sample matrices to ensure accurate and reliable detection.

Determination of ambroxol in urine samples: The sensor was applied to detect ambroxol in spiked urine samples. Urine (5 mL) was diluted to 25 mL with supporting electrolyte and different concentrations of ambroxol (4-12 mg) were added. Voltammograms were recorded and the concentrations of unknown samples were determined using the calibration curve. The average percentage recovery of ambroxol in urine was found to be 100.9%, demonstrating the practical applicability of the developed sensor (Table-2).

Conclusion

This study successfully demonstrates the green synthesis of silver nanoparticles (AgNPs) using *Hyphaene thebaica* extract and their integration with MWCNTs and Nafion to fabricate a high-performance electrochemical sensor for the detection of ambroxol drug. The characterization confirmed the crystalline nature of the AgNPs, their irregular morphology, and the stabilizing role of phytochemicals. The AgNPs/MWCNT/Nafion-modified GCE exhibited superior electrochemical activity compared to bare and Nafion-modified electrodes, with enhanced peak currents, increased effective surface area and improved electron transfer. Optimization of analytical parameters, including pH, accumulation time, nanoparticle dispersion and scan rate, resulted in high sensitivity, reproducibility and selectivity. The sensor maintained reliable performance in the presence of various potential interferents and successfully quantified ambroxol in spiked urine samples with near-complete recovery, demonstrating its practical applicability.

CONFLICT OF INTEREST

The authors declare that there is no conflict of interests regarding the publication of this article.

DECLARATION OF AI-ASSISTED TECHNOLOGIES

During the preparation of this manuscript, the authors used an AI-assisted tool(s) to improve the language. The authors reviewed and edited the content and take full responsibility for the published work.

REFERENCES

1. Y. Fang, H. Chang, J. Li, Z. Li and D. Zhang, *Crit. Rev. Anal. Chem.*, **54**, 1680 (2024); https://doi.org/10.1080/10408347.2022.2128633
2. S.-A. Leau, C. Lete and S. Lupu, *Chemosensors*, **11**, 179 (2023); https://doi.org/10.3390/chemosensors11030179
3. Y. Torlak, E.E. Altuner, Y. Tekeli and T. Tekeli, *J. Pharm. Res. Int.*, **37**, 34 (2025); https://doi.org/10.9734/jpri/2025/v37i117765
4. M. Imran, S. Ahmed, A.Z. Abdullah, J. Hakami, A.A. Chaudhary, H.A. Rudayni, S.-U.-D. Khan, A. Khan and N.S. Basher, *Luminescence*, **38**, 1064 (2023); https://doi.org/10.1002/bio.4408
5. M.A. Darwish, W. Abd-Elaziem, A. Elsheikh and A.A. Zayed, *Nanoscale Adv.*, **6**, 4015 (2024); https://doi.org/10.1039/D4NA00214H
6. M. Harun-Ur-Rashid, A.B. Imran and T. Foyez, *Discov. Electrochem.*, **2**, 14 (2025); https://doi.org/10.1007/s44373-025-00027-9
7. K. Patzwaldt and S. Castaneda-Vega, *Neural Regen. Res.*, **19**, 2345 (2024); https://doi.org/10.4103/NRR.NRR-D-23-01664
8. A. Kantar, L. Klimek, D. Cazan, A. Sperl, U. Sent and M. Mesquita, *Multidiscip. Respir. Med.*, **15**, 511 (2020); https://doi.org/10.4081/mrm.2020.511
9. D. Cazan, L. Klimek, A. Sperl, M. Plomer and S. Kölsch, *Expert Opin. Drug Saf.*, **17**, 1211 (2018); https://doi.org/10.1080/14740338.2018.1533954
10. P.D. Sonawane, S.R. Chaudhari, S.B. Ganorkar, A.S. Patil and A.A. Shirkhedkar, *Anal. Biochem.*, **657**, 114888 (2022); https://doi.org/10.1016/j.ab.2022.114888
11. W. Parys, M. Dołowy, and A. Pyka-Pająk, *Processes*, **10**, 172 (2022); https://doi.org/10.3390/pr10010172
12. R. Kumar, S. Salwan, P. Kumar, N. Bansal and B. Kumar, *Analytica*, **6**, 12 (2025); https://doi.org/10.3390/analytica6020012
13. A. Haghighizadeh, F. Abdolabadi, M. Amirinejad, S. Dadpour and O. Rajabi, *ChemistrySelect*, **10**, e01067 (2025); https://doi.org/10.1002/slct.202501067

14. A. Kumar, M.R.S. Savanur, S.K. Singh, J. Singh, S. Bhattacharya, K. Asnani, B. Kumar, M. Kumar and S. Kumar, *ChemistrySelect*, **10**, e202403655 (2025); https://doi.org/10.1002/slct.202403655
15. R.K. Sharma, S. Yadav, S. Dutta, H.B. Kale, I.R. Warkad, R. Zbořil, R.S. Varma and M.B. Gawande, *Chem. Soc. Rev*., **50**, 11293 (2021); https://doi.org/10.1039/D0CS00912A
16. J. Tang, R. Li, S. Mahmood, J. Li and S. Yao, *Chemosensors*, **13**, 367 (2025); https://doi.org/10.3390/chemosensors13100367
17. R.M. Kakhki, *Int. J. Polym. Mater. Polym. Biomater*., **73**, 1470 (2024); https://doi.org/10.1080/00914037.2023.2297436
18. S. Ahmed, Saifullah, M. Ahmad, B.L. Swami and S. Ikram, *J. Radiat. Res. Appl. Sci.*, **9**, 1 (2016); https://doi.org/10.1016/j.jrras.2015.06.006
19. S. Iravani, *Green Chem.*, **13**, 2638 (2011); https://doi.org/10.1039/C1GC15386B
20. P. Prakash, P. Gnanaprakasam, R. Emmanuel, S. Arokiyaraj and M. Saravanan, *Mater. Lett*., **97**, 141 (2013); https://doi.org/10.1016/j.matlet.2013.01.087
21. W. Dagher, A. Alassod, M.F. Al Hinnawi, I. Alghoraibi, A. Taher and M. Alnhlaouie, *RSC Adv*., **15**, 35642 (2025); https://doi.org/10.1039/D5RA05214A
22. S. Haq, K. A. Yasin, W. Rehman, M. Waseem, M. N. Ahmed, M. I. Shahzad, N. Shahzad, A. Shah, M. U. Rehman and B. Khan, *J. Inorg. Organomet. Polym*., **31**, 1134 (2021); https://doi.org/10.1007/s10904-020-01763-8
23. I. Anshori, L.R. Ula, G.I.N. Asih, E. Ariasena, U. Uperianti, A.N. Raditya, Y. Mulyaningsih, M. Handayani, A. Purwidyantri and B.A. Prabowo, *Nanotechnology*, **35**, 115501 (2023); https://doi.org/10.1088/1361-6528/ad143f
24. J. Natsuki and T. Natsuki, *Nanotechnology*, **13**, 1297 (2023); https://doi.org/10.3390/nano13081297
25. T.E. Mpanza, M.Sc. Dissertation, Determination of Capsaicin using Carbon Nanotube Based Electrochemical Biosensors, Department of Applied Science in Chemistry, Faculty of Applied Sciences, Durban University of Technology, South Africa (2016).
26. K.A.M. Attia, A.M. Abdel-Raoof, A. Serag, S.M. Eid and A.E. Abbas, *RSC Adv.*, **12**, 17536 (2022); https://doi.org/10.1039/D2RA01962K
27. Y. Piao, *Int. J. Electrochem. Sci*., **7**, 6084 (2012); https://doi.org/10.1016/S1452-3981(23)19463-6
28. F.M. Abdel-Haleem, E. Gamal, M.S. Rizk, A. Madbouly, R.M. El Nashar, B. Anis, H.M. Elnabawy, A.S.G. Khalil and A. Barhoum, *Front. Bioeng. Biotechnol*., **9**, 648704 (2021); https://doi.org/10.3389/fbioe.2021.648704